Perturbative QCD

W. J. Stirling

Departments of Mathematical Sciences and Physics,
University of Durham, Durham, England.

Abstract

Some of the basic concepts and most important results of perturbative QCD are presented, together with some illustrative comparisons with experiment.

1 The QCD Lagrangian

The QCD Lagrangian is, up to gauge-fixing terms,

$$
\begin{aligned}
\mathcal{L}_{QCD} &= -\frac{1}{4}F^{(a)}_{\mu\nu}F^{(a)\mu\nu} + \sum_q \bar{\psi}^q_i(i\gamma^\mu(D_\mu)_{ij} - m_q\delta_{ij})\psi^q_j \\
F^{(a)}_{\mu\nu} &= \partial_\mu A^a_\nu - \partial_\nu A^a_\mu + g_s f_{abc}A^b_\mu A^c_\nu \\
(D_\mu)_{ij} &= \delta_{ij}\partial_\mu - ig_s T^a_{ij}A^a_\mu
\end{aligned}
\tag{1}
$$

where g_s is the QCD coupling constant, T^a_{ij} and f_{abc} are the SU(3) colour matrices and structure constants respectively, the $\psi^q_i(x)$ are the 4-component Dirac spinors associated with each quark field of colour i and flavour q, and the $A^a_\mu(x)$ are the eight Yang-Mills gluon fields.

2 Colour Matrix Identities

Explicit forms for the SU(3) colour matrices and structure constants can be found, for example, in the *Review of Particle Properties* [1]. The following are some useful identities:

$$
\begin{aligned}
[T^a, T^b] &= if^{abc}T^c \\
\{T^a, T^b\} &= d^{abc}T^c + \frac{1}{3}\delta^{ab} \\
f^{acd}f^{bcd} &= C_A\delta^{ab} \\
(T^aT^a)_{ij} = T^a_{ik}T^a_{kj} &= C_F\delta_{ij} \\
\mathrm{Tr}(T^aT^b) = T^a_{ij}T^b_{ji} &= T_F\delta^{ab} \\
C_A &= N_c = 3 \\
C_F &= \frac{N_c^2-1}{2N_c} = \frac{4}{3} \\
T_F &= \frac{1}{2} \\
\mathrm{Tr}(T^aT^bT^c) &= \frac{i}{4}f^{abc} + \frac{1}{4}d^{abc} \\
f^{abc}f^{abc} &= 24 \\
d^{abc}d^{abc} &= \frac{40}{3}
\end{aligned}
\tag{2}
$$

where summation over repeated indices is understood.

3 The QCD Coupling Constant

The scale dependence of the renormalized QCD coupling $\alpha_s \equiv g_s^2/4\pi$ is determined by the β-function coefficients:

$$\begin{aligned}
\frac{\mu^2}{\alpha_s(\mu^2)}\frac{\partial\alpha_s(\mu^2)}{\partial\mu^2} &= -\frac{\alpha_s(\mu^2)}{4\pi}\beta_0 - (\frac{\alpha_s(\mu^2)}{4\pi})^2\beta_1 - (\frac{\alpha_s(\mu^2)}{4\pi})^3\beta_2 + ... \\
\beta_0 &= 11 - \frac{2}{3}n_f \\
\beta_1 &= 102 - \frac{38}{3}n_f \\
\beta_2(\overline{\mathrm{MS}}) &= \frac{2857}{2} - \frac{5033}{18}n_f + \frac{325}{54}n_f^2.
\end{aligned} \tag{3}$$

Retaining only the first two terms on the right hand side and solving the differential equation for $\alpha_s(\mu^2)$ gives

$$\frac{1}{\alpha_s} + b_1 \log\Big(\frac{b_1\alpha_s}{1+b_1\alpha_s}\Big) = b_0 \log\frac{\mu^2}{\Lambda^2}, \tag{4}$$

with

$$b_0 = \frac{\beta_0}{4\pi}, \quad b_1 = \frac{\beta_1}{4\pi\beta_0}. \tag{5}$$

Note that a constant of integration in the form of a dimensionful parameter Λ has been introduced – replacing Λ by $c\Lambda$ also gives a solution to the differential equation. The convention chosen here is such that the left hand side vanishes when $\mu = \Lambda$. This is the standard definition of the 'two-loop' coupling constant as a function of the scale μ and the fundamental QCD scale parameter Λ. It is adequate for 'next-to-leading order' phenomenology. The above expression for α_s can be generalized to include also the β_2 term [2].

An explicit form for α_s can be obtained by expanding in inverse powers of $\log(\mu^2/\Lambda^2)$:

$$\alpha_s(\mu^2) = \frac{12\pi}{(33-2n_f)\log(\mu^2/\Lambda^2)}\Big[1 - \frac{6(153-19n_f)}{(33-2n_f)^2}\frac{\log\log(\mu^2/\Lambda^2)}{\log(\mu^2/\Lambda^2)} + ...\Big], \tag{6}$$

which illustrates the characteristic 'asymptotic freedom' property – the coupling decreases monotonically as μ^2 increases. Note however that this expansion corresponds to a slightly different definition of Λ from the implicit expression (4) for α_s, the expansion of which would contain a term $\sim$ const./$\log^2$. The freedom to multiply Λ by a constant can be used to remove this term. There is a $\mathcal{O}(15\%)$

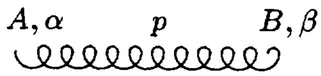

$$\delta^{AB}\left[-g^{\alpha\beta}+(1-\lambda)\frac{p^\alpha p^\beta}{p^2+i\varepsilon}\right]\frac{i}{p^2+i\varepsilon}$$

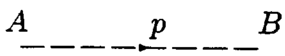

$$\delta^{AB}\frac{i}{p^2+i\varepsilon}$$

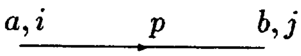

$$\delta^{ab}\frac{i}{(\hat{p}-m+i\varepsilon)_{ji}}$$

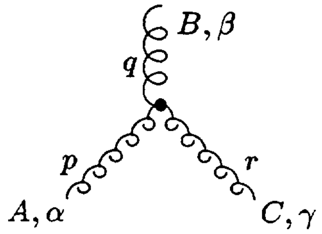

$$-gf^{ABC}\left[g^{\alpha\beta}(p-q)^\gamma+g^{\beta\gamma}(q-r)^\alpha+g^{\gamma\alpha}(r-p)^\beta\right]$$

(all momenta incoming)

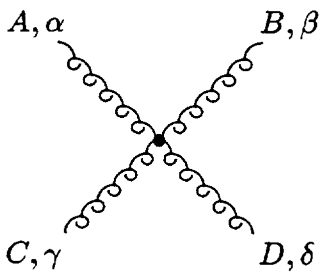

$$\begin{aligned}&-ig^2 f^{XAC}f^{XBD}\left(g_{\alpha\beta}g_{\gamma\delta}-g_{\alpha\delta}g_{\beta\gamma}\right)\\&-ig^2 f^{XAD}f^{XBC}\left(g_{\alpha\beta}g_{\gamma\delta}-g_{\alpha\gamma}g_{\beta\delta}\right)\\&-ig^2 f^{XAB}f^{XCD}\left(g_{\alpha\gamma}g_{\beta\delta}-g_{\alpha\delta}g_{\beta\gamma}\right)\end{aligned}$$

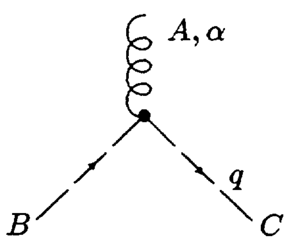

$$gf^{ABC}q^\alpha$$

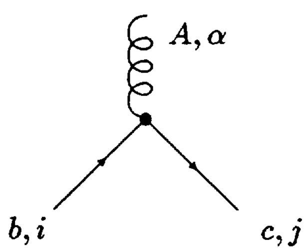

$$-ig\left(t^A\right)_{cb}(\gamma^\alpha)_{ji}$$

Table 1: Feynman rules for QCD in a covariant gauge.

$\Lambda^{(5)}_{\overline{\rm MS}}$ (MeV)	$\alpha_s(M_Z^2)$
50	0.0970
100	0.1060
150	0.1122
200	0.1170
250	0.1210
300	0.1245
350	0.1277
400	0.1305
450	0.1332
500	0.1356
550	0.1379
600	0.1401

Table 2: $\alpha_s(M_Z^2)$ for various $\Lambda^{(5)}_{\overline{\rm MS}}$.

difference in the Λ's defined by (4) and (6). Since in practice it is usually α_s which is measured experimentally, it is important when comparing Λ values to check that the same equation has been used to determine Λ from the coupling constant.

A second difficulty with the above definitions is that Λ depends on the number of active flavours. Values of Λ for different numbers of flavours are defined by imposing the continuity of α_s at the scale $\mu = m$, where m is the mass of the heavy quark. For example, for the b-quark threshold: $\alpha_s(m_b^2, 4) = \alpha_s(m_b^2, 5)$. Using the next-to-leading order form (4) for $\alpha_s(Q^2)$ one can show that

$$\Lambda(4) \approx \Lambda(5)\Big(\frac{m_b}{\Lambda(5)}\Big)^{\frac{2}{25}}\Big[\ln\Big(\frac{m_b^2}{\Lambda(5)^2}\Big)\Big]^{\frac{963}{14375}}. \tag{7}$$

In practice, most higher order QCD corrections are carried out using the *modified minimal subtraction* ($\overline{\rm MS}$) regularization scheme. To be consistent, then, one uses the above results for $\alpha_s(\mu^2)$ with $\Lambda \equiv \Lambda_{\overline{\rm MS}}$.

Some recent α_s measurements are shown in Fig.1. The lines indicate different values of $\Lambda^{(5)}_{\overline{\rm MS}}$. Extreme caution should be exercised when comparing the precision of the various measurements, as the errors have different meanings in different processes. A central value of $\Lambda^{(5)}_{\overline{\rm MS}} \simeq 150$ MeV is indicated. With the advent of high precision measurements of α_s at LEP, one can nowadays take $\alpha_s(M_Z^2)$ as the fundamental parameter of QCD, rather than $\Lambda_{\overline{\rm MS}}$. Table 2 gives the conversion between $\Lambda^{(5)}_{\overline{\rm MS}}$ and $\alpha_s(M_Z^2)$ using the definition given in eqn.(4).

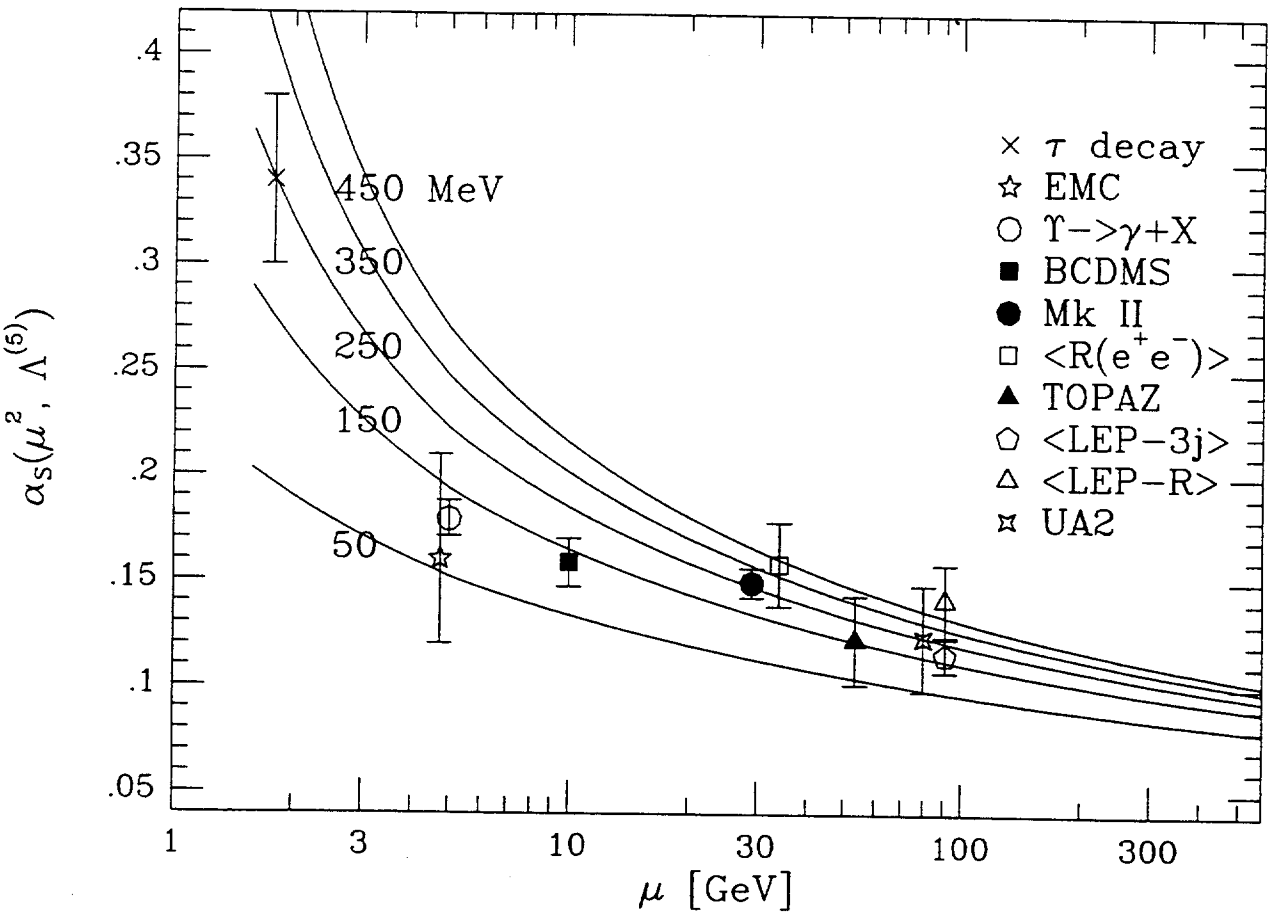

Figure 1: A compilation of α_s measurements from different processes.

4 Deep Inelastic Scattering

Consider the deep inelastic process $lp \to lX$. Label the incoming and outgoing lepton four-momenta by k^μ and k'^μ respectively, the incoming proton momentum by p^μ ($p^2 = M^2$) and the momentum transfer by $q^\mu = k^\mu - k'^\mu$. The standard deep inelastic variables are defined by:

$$
\begin{aligned}
Q^2 &= -q^2 \qquad p^2 = M^2 \\
x &= \frac{Q^2}{2p\cdot q} = \frac{Q^2}{2M(E-E')} \\
y &= \frac{q\cdot p}{k\cdot p} = 1 - E'/E \\
s &= (k+p)^2 = M^2 + \frac{Q^2}{xy},
\end{aligned}
\tag{8}
$$

where the energies are defined in the rest frame of the target. The structure functions $F_i(x, Q^2)$ are then defined in terms of the lepton scattering cross sections. For charged lepton scattering, $lp \to lX$,

$$
\begin{aligned}
\frac{d^2\sigma^{em}}{dxdy} &= \frac{4\pi\alpha^2(s-M^2)}{Q^4}\Big[\Big(\frac{1+(1-y)^2}{2}\Big)2xF_1^{em} \\
&\quad +(1-y)(F_2^{em} - 2xF_1^{em}) - \frac{M^2}{s-M^2}xyF_2^{em}\Big],
\end{aligned}
\tag{9}
$$

and for neutrino (antineutrino) scattering, $\nu(\bar\nu)p \to lX$,

$$
\begin{aligned}
\frac{d^2\sigma^{\nu(\bar\nu)}}{dxdy} &= \frac{G_F^2(s-M^2)}{2\pi}\Big[(1 - y - \frac{M^2}{s-M^2}xy)F_2^{\nu(\bar\nu)} \\
&\quad + y^2xF_1^{\nu(\bar\nu)} + (-)y(1-y/2)xF_3^{\nu(\bar\nu)}\Big].
\end{aligned}
\tag{10}
$$

In the quark-parton model, these structure functions are related to the quark 'distribution functions' or 'densities' $q(x, Q^2)$, where $q(x, Q^2)dx$ is the probability that a parton carries a momentum fraction x of the target nucleon's momentum when probed (by a gauge boson γ^*, W or Z) at energy scale Q. Thus

$$
\begin{aligned}
F_2^\nu &= 2x[d + s + \bar u + \bar c] \\
xF_3^\nu &= 2x[d + s - \bar u - \bar c] \\
F_2^{\bar\nu} &= 2x[u + c + \bar d + \bar s] \\
xF_3^{\bar\nu} &= 2x[u + c - \bar d - \bar s] \\
F_2^{em} &= x[\frac{4}{9}(u + u + c + \bar c) + \frac{1}{9}(d + \bar d + s + \bar s)] \\
2xF_1 &= F_2.
\end{aligned}
\tag{11}
$$

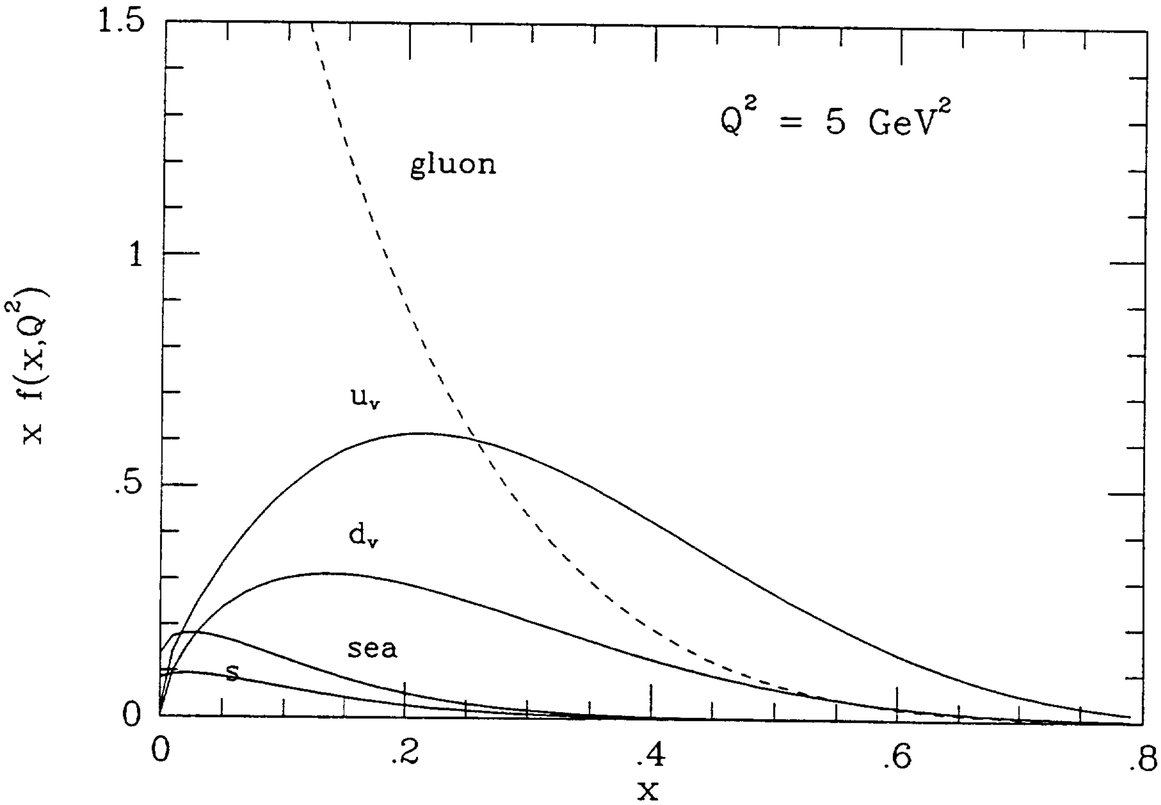

Figure 2: Quark and gluon distributions at $Q^2 = 5\ \mathrm{GeV}^2$ from reference [3].

Note that when the nature of the target is unambiguous the notation $q(x, Q^2)$ and $G(x, Q^2)$ for the quark and gluon densities can be used, otherwise a general notation is $f_{a/A}(x, Q^2)$, where a = u, d, ... g and A = p, n, Fe, Cu, etc.

Fig.2 shows some representative quark and gluon distributions (the KMRS(B0) distributions of reference [3]) extracted from deep inelastic scattering and other processes. Note that 'sea' refers to the (equal) $\bar{u}$ and $\bar{d}$ distributions in the proton.

5 Scaling Violations – the Altarelli-Parisi Equations

In the 'naive' parton model the structure functions *scale*, i.e. $F(x, Q^2) \rightarrow F(x)$ in the asymptotic (Bjorken) limit: $Q^2 \rightarrow \infty$, x fixed. In QCD, this scaling is *broken* by logarithms of Q^2. In describing the way in which scaling is violated it is convenient to define singlet and non-singlet quark distributions:

$$F^{NS} = q_i - q_j, \qquad F^S = \sum_i (q_i + \bar{q}_i). \tag{12}$$

The non-singlet structure functions have non-zero values of flavour quantum numbers such as isospin or baryon number. The variation with Q^2 of these functions is described by the so-called Altarelli-Parisi equations [4]:

$$\begin{aligned} Q^2\frac{\partial F^{NS}}{\partial Q^2} &= \frac{\alpha_s(Q^2)}{2\pi}P^{qq} * F^{NS} \\ Q^2\frac{\partial F^{S}}{\partial Q^2} &= \frac{\alpha_s(Q^2)}{2\pi}(P^{qq} * F^{S} + 2n_f P^{qg} * G) \\ Q^2\frac{\partial G}{\partial Q^2} &= \frac{\alpha_s(Q^2)}{2\pi}(P^{gq} * F^{S} + P^{gg} * G), \end{aligned} \tag{13}$$

where $*$ denotes a convolution integral:

$$f * g = \int_x^1 \frac{dy}{y} f(y) g(\frac{x}{y}). \tag{14}$$

In leading order the Altarelli-Parisi splitting functions are

$$\begin{aligned} P^{qq} &= \frac{4}{3}\Big(\frac{1+x^2}{1-x}\Big)_+ \\ P^{qg} &= \frac{1}{2}(x^2 + (1-x)^2) \\ P^{gq} &= \frac{4}{3}\Big(\frac{1+(1-x)^2}{x}\Big) \\ P^{gg} &= 6\Big(\frac{1-x}{x} + x(1-x) + (\frac{x}{1-x})_+\Big) \\ &\quad -(\frac{1}{2} + \frac{n_f}{3})\delta(1-x). \end{aligned} \tag{15}$$

Note the 'plus prescription' for the functions which are singular as $x \to 1$:

$$\int_0^1 dx f(x)(g(x))_+ = \int_0^1 dx(f(x) - f(1))g(x). \tag{16}$$

The Altarelli-Parisi equations can be solved analytically by defining *moments* (formally, the Mellin transforms) of the structure functions, $M_n^{NS} =< F^{NS} >_n \equiv \int_0^1 dx x^{n-1} F^{NS}$ etc. The convolution integral then becomes a simple product. Introducing the leading order expression for the QCD coupling constant (see above),

$$\alpha_s(Q^2) = \frac{4\pi}{\beta_0 \log(Q^2/\Lambda^2)}, \tag{17}$$

one obtains, for the non-singlet solution,

$$M_n^{NS}(Q^2) = M_n^{NS}(Q_0^2)\left(\frac{\alpha_s(Q^2)}{\alpha_s(Q_0^2)}\right)^{-d_n}, \tag{18}$$

where $d_n = 2 < P^{qq} >_n / \beta_0$. Note that $d_1 = 0$ and that $d_n <` 0$ for $n \geq 2$, which implies that the x distributions decrease and increase with increasing Q^2 at large and small x respectively. Solutions for the singlet and gluon moments can be found in a similar way, by first diagonalizing the coupled equations.

The precision of contemporary deep inelastic data demands that the QCD predictions are calculated to next-to-leading order. This amounts to the replacements (shown schematically):

$$\begin{aligned} P(x) &\rightarrow P^{(0)}(x) + \frac{\alpha_s}{2\pi} P^{(1)}(x) \\ F = \sum q &\rightarrow F^{(1)} = \sum C * q, \qquad C = \delta(1-x) + O(\alpha_s). \end{aligned} \tag{19}$$

An example of a next-to-leading order QCD fit [3] to recent high-precision data on $F_2^{\mu D}$ from the BCDMS collaboration [5] is shown in Fig.3.

6 Hard Processes in Hadronic Collisions

A fundamental theorem of QCD states that if there is a large momentum transfer in the quark or gluon scattering subprocess (here 'large' generally means much greater than the QCD scale Λ) then hadronic cross sections can be expressed as a convolution of universal parton distributions, measurable for example in deep inelastic scattering, and a subprocess cross section calculable in principle to arbitrary order in strong or electroweak perturbation theory:

$$\sigma^{AB\rightarrow X+\ldots} = \sum_{a,b=q,g} \int_0^1 dx_a dx_b \; f_{a/A}(x_a, Q^2) f_{b/B}(x_b, Q^2) \cdot \hat{\sigma}^{ab\rightarrow X}|_{\hat{s}=x_a x_b s_{AB}} \tag{20}$$

with the factorization scale Q usually taken to be a 'typical' energy for the subprocess. The general expression for a scattering cross section is given in Appendix A. Some specific examples are given below.

(a) Drell-Yan, W and Z production cross sections are obtained from the subprocess cross sections:

$$\frac{d\hat{\sigma}^{\,q\bar{q}\rightarrow l^+l^-}}{dM^2} = \frac{4\pi\alpha^2}{9M^2} e_q^2 \delta(\hat{s} - M^2)$$

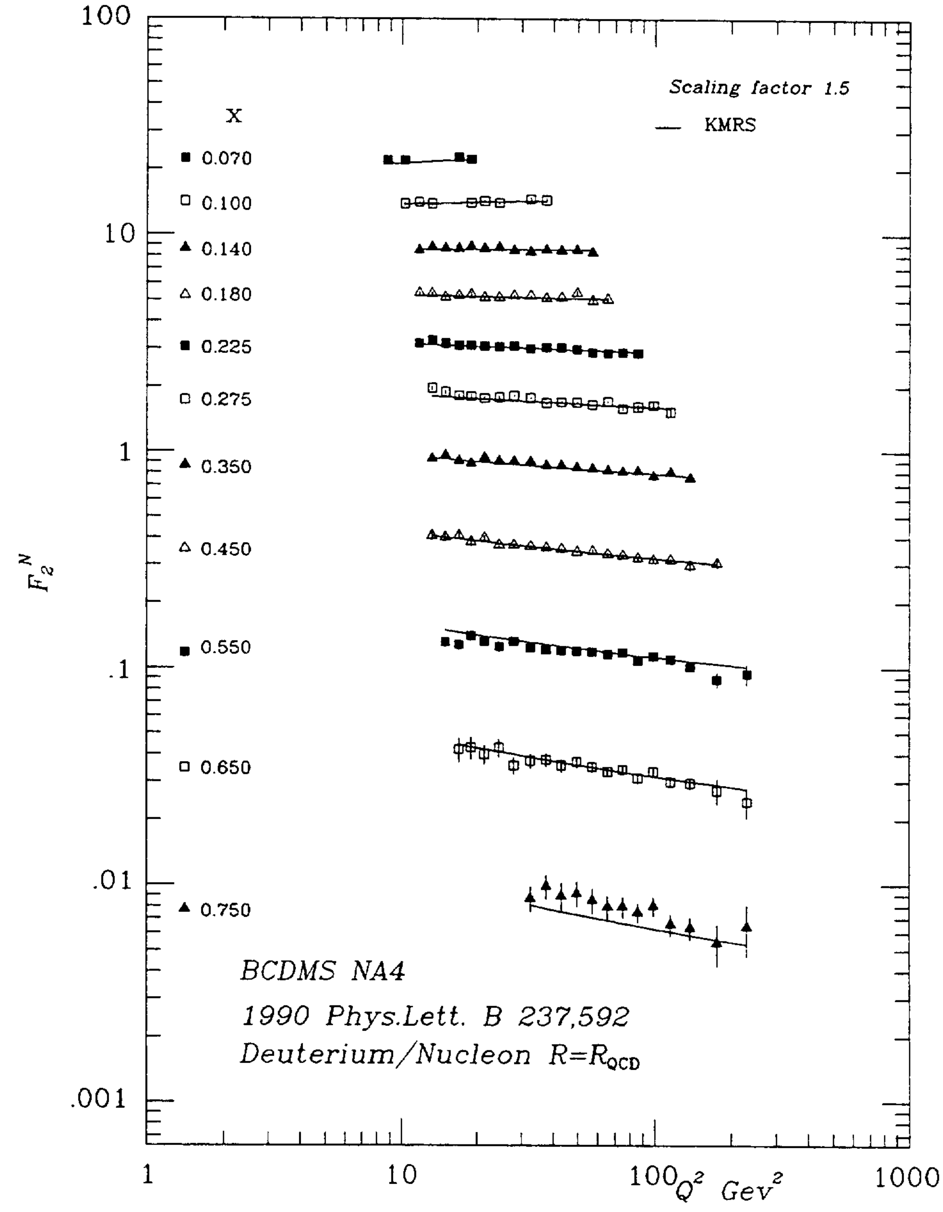

Figure 3: Next-to-leading order QCD fit to $F_2^{\mu D}$ [5] from reference [3].

$$\begin{aligned}
\hat{\sigma}^{q\bar{q}\to Z} &= \frac{4\pi\alpha}{3}\frac{v_q^2+a_q^2}{4\sin^2\theta_W\cos^2\theta_W}\,\delta(\hat{s}-M_Z^2)\\
\hat{\sigma}^{q\bar{q}'\to W} &= \frac{4\pi\alpha}{3}\frac{1}{4\sin^2\theta_W}\,\delta(\hat{s}-M_W^2),
\end{aligned}\tag{21}$$

where the (v_f, a_f) couplings are, for different fermion types,

$$\begin{array}{ll}
\nu_e & (\frac{1}{2},\frac{1}{2})\\
e^- & (-\frac{1}{2}+2\sin^2\theta_W,-\frac{1}{2})\\
u & (\frac{1}{2}-\frac{4}{3}\sin^2\theta_W,\frac{1}{2})\\
d & (-\frac{1}{2}+\frac{2}{3}\sin^2\theta_W,-\frac{1}{2}).
\end{array}\tag{22}$$

(b) For the production of a pair of heavy quarks of mass M:

$$\begin{aligned}
\hat{\sigma}^{q\bar{q}\to Q\bar{Q}} &= \frac{\pi\alpha_s^2\beta\rho}{27M^2}(2+\rho)\\
\hat{\sigma}^{gg\to Q\bar{Q}} &= \frac{\pi\alpha_s^2\beta\rho}{192M^2}\Big[\frac{1}{\beta}(\rho^2+16\rho+16)\log\frac{1+\beta}{1-\beta}-28-31\rho\Big],
\end{aligned}\tag{23}$$

where $\rho = 4M^2/\hat{s}$, $\beta = \sqrt{1-\rho}$.

(c) Two important Higgs production mechanisms are

$$\hat{\sigma}^{gg\to H} = \frac{\alpha\alpha_s^2 M_H^2}{576\sin^2\theta_W M_W^2}\left|I\left(\frac{m_t^2}{M_H^2}\right)\right|^2 \tag{24}$$

where $I(x)$ is a dimensionless function given by

$$\begin{aligned}
I(x) &= 3x[2+(4x-1)F(x)]\\
F(x) &= \theta(1-4x)\frac{1}{2}\left[\log\left(\frac{1+\sqrt{1-4x}}{1-\sqrt{1-4x}}\right)-i\pi\right]^2-\theta(4x-1)2\left[\sin^{-1}(1/2\sqrt{x})\right]^2,
\end{aligned}\tag{25}$$

and

$$\hat{\sigma}^{q\bar{q}'\to WH} = \frac{\pi\alpha^2}{36\sin^4\theta_W}\frac{2p}{\sqrt{\hat{s}}}\frac{p^2+3M_W^2}{(\hat{s}-M_W^2)^2},\quad p=\frac{\lambda^{\frac{1}{2}}(\hat{s},M_W^2,M_H^2)}{2\sqrt{\hat{s}}} \tag{26}$$

(d) The *inclusive jet cross section* in hadronic collisions is given, to leading order, by

$$\begin{aligned}
E_J\frac{d\sigma}{d^3p_J} &= \sum_{a,b,c,d=q,g}\int_0^1 dx_a dx_b\, f_{a/A}(x_a,Q^2)f_{b/B}(x_b,Q^2)\\
&\quad\cdot\delta(\hat{s}+\hat{t}+\hat{u})\frac{1}{16\pi^2\hat{s}}|\overline{M}^{ab\to cd}|^2,
\end{aligned}\tag{27}$$

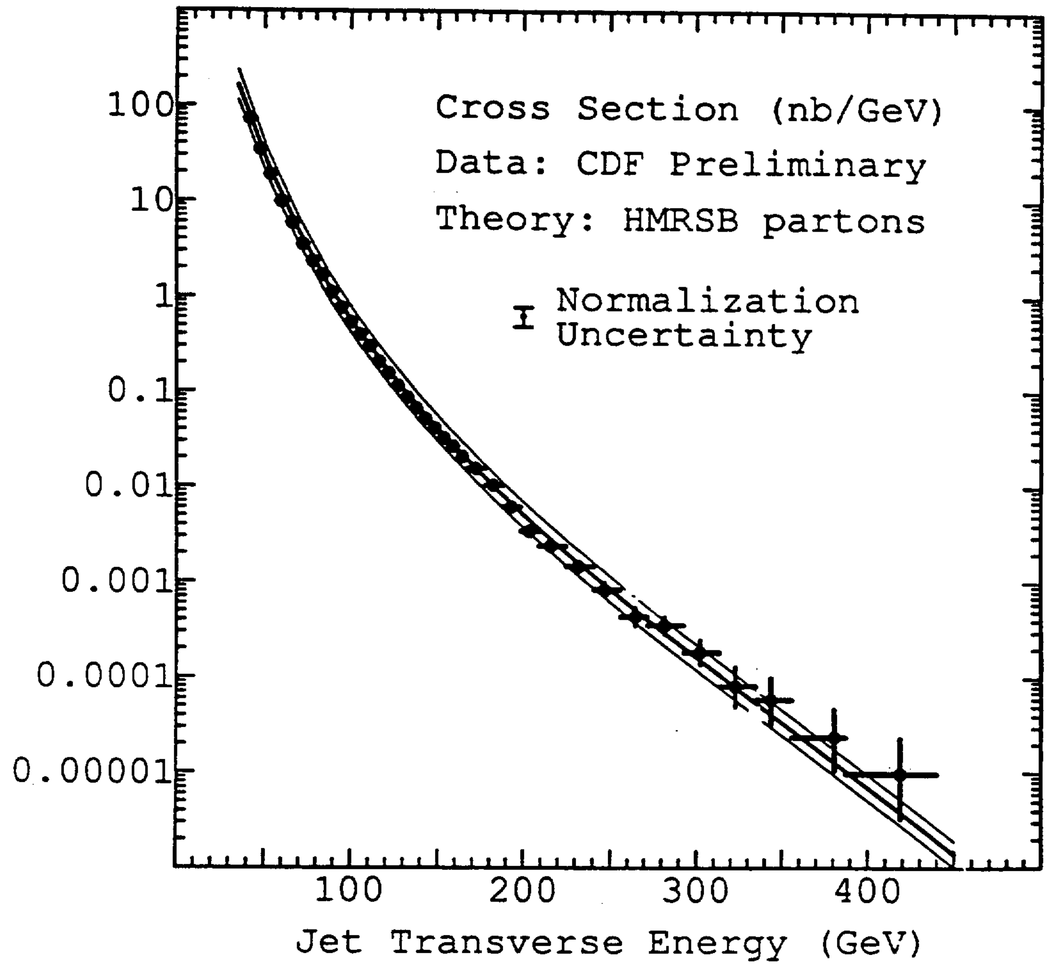

Figure 4: The jet inclusive cross in next-to-leading order QCD, from reference [10].

with $\hat{s}$, $\hat{t}$, $\hat{u}$ the Mandelstam invariants for the subprocess, and the bar on the scattering amplitude denotes a spin and colour sum/average. Note that this result corresponds to massless quarks and gluons and that no distinction is made between quark and gluon jets. A complete list of all the $2 \to 2$ scattering matrix elements is given in Appendix B.

The next-to-leading order QCD corrections to all the above processes (a) – (d) have been calculated [6,7,8,9,10]. Where data are available, the agreement between theory and experiment is excellent. As an example, Fig.4 shows a comparison of data from the CDF collaboration on the inclusive jet cross section in $p\bar{p}$ collisions at $\sqrt{s} = 1800$ GeV with the NLO predictions from S.D. Ellis *et al.* [10].

7 QCD in High Energy e^+e^- Collisions

7.1 The Total Hadronic Cross Section

The total hadronic cross section is obtained from the cross section for e^+e^- annihilation into quark and gluon final states. Thus, ignoring weak effects and treating all quarks as massless,

$$\begin{aligned}
\sigma_{tot} &= \frac{4\pi\alpha^2}{3s} R, \\
R &= K_{QCD}\, 3\sum_q e_q^2, \\
K_{QCD} &= 1 + \sum_{n\geq 1} C_n\left(\frac{\alpha_s}{\pi}\right)^n. \qquad (28)
\end{aligned}$$

The coefficients C_1, C_2 and C_3 have been calculated – they are (in the $\overline{\rm MS}$ scheme with the renormalization scale choice $\mu = \sqrt{s}$):

$$\begin{aligned}
C_1 &= 1 \\
C_2 &= \left(\frac{2}{3}\zeta(3) - \frac{11}{12}\right)n_f + \left(\frac{365}{24} - 11\zeta(3)\right) \\
&\simeq 1.986 - 0.115 n_f \\
C_3 &= \left(\frac{87029}{288} - \frac{1103}{4}\zeta(3) + \frac{275}{6}\zeta(5)\right) \\
&\quad -\left(\frac{7847}{216} - \frac{262}{9}\zeta(3) + \frac{25}{9}\zeta(5)\right)n_f \\
&\quad +\left(\frac{151}{162} - \frac{19}{27}\zeta(3)\right)n_f^2 \\
&\quad -\frac{\pi^2}{432}(33 - 2n_f)^2 + \eta\left(\frac{55}{72} - \frac{5}{3}\zeta(3)\right) \\
&\simeq -6.637 - 1.200 n_f - 0.005 n_f^2 - 1.240\eta, \qquad (29)
\end{aligned}$$

where $\eta = (\sum_f Q_f)^2/3\sum_f Q_f^2$. The result for C_3 is taken from reference [11]. Apart from the η term, the result for the QCD corrections K is the same for the ratio of hadronic to leptonic Z decay widths: $R_Z = \Gamma_h/\Gamma_\mu$. In practice, quark masses (particularly m_b and m_t) have a non-negligible effect [12] and must be taken into account in precision fits to data [13].

Through $\mathcal{O}(\alpha_s^3)$ the μ dependence is restored by the replacements:

$$\alpha_s \rightarrow \alpha_s(\mu^2)$$

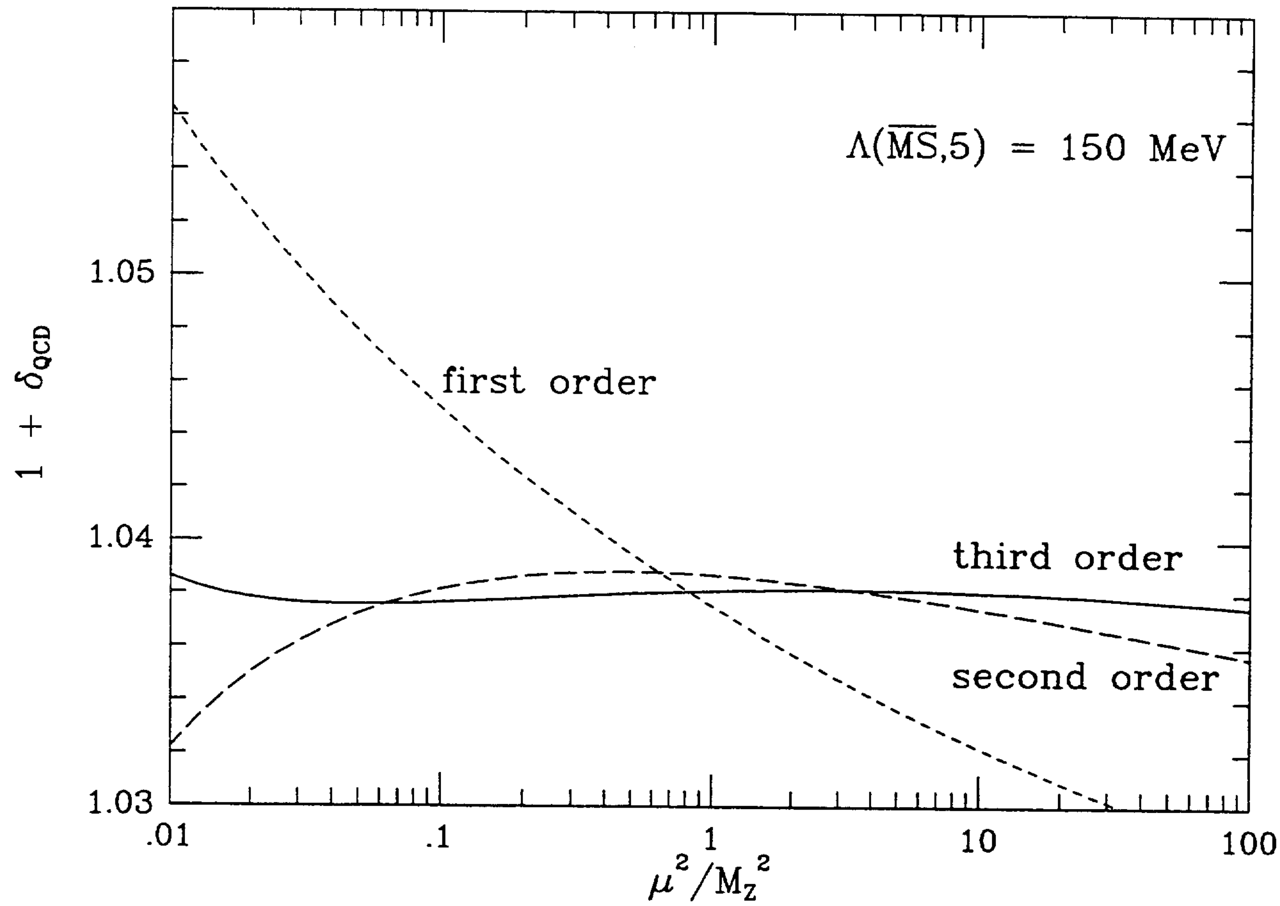

Figure 5: The effect of higher order QCD corrections to R_Z, as a function of the renormalization scale μ.

$$\begin{aligned} C_2 &\rightarrow C_2 - C_1\frac{\beta_0}{4}\log\frac{s}{\mu^2} \\ C_3 &\rightarrow C_3 + C_1\left(\frac{\beta_0}{4}\right)^2\log^2\frac{s}{\mu^2} - (C_1\frac{\beta_1}{16} + C_2\frac{\beta_0}{2})\log\frac{s}{\mu^2}. \end{aligned} \tag{30}$$

where β_0 and β_1 are defined in Section 3. The all-orders prediction is independent of the renormalization scheme (equivalently, independent of μ in the $\overline{\mathrm{MS}}$ convention). Truncated series such as the one above *are* dependent on μ, but this dependence becomes weaker the more terms are included in the series. This is illustrated in Fig.5, which shows $K_{QCD} = 1 + \delta$ for R_Z as a function of μ, as the higher order terms are added in.

7.2 Three Jet Cross Section in e^+e^- Annihilation

Consider the next-to-leading process $e^+e^- \rightarrow q\bar{q}g$. Define x_1, x_2 and x_3 to be the energy, in the e^+e^- centre-of-mass frame, of the final state quark, antiquark and gluon respectively, normalized to the beam energy, *i.e.* $x_i = 2E_i/\sqrt{s}$, $\sum x_i = 2$. The differential cross section is then

$$\frac{1}{\sigma}\frac{d^2\sigma}{dx_1 dx_2} = \frac{2\alpha_s}{3\pi}\frac{x_1^2 + x_2^2}{(1-x_1)(1-x_2)}. \tag{31}$$

For scalar gluons, $x_1^2 + x_2^2$ is replaced by $x_3^2/2$.

A three-jet fraction can be defined by requiring that $s_{ij} = (1-x_k)s > ys$ (JADE algorithm [14]) and integrating the above differential distribution over the appropriate region gives

$$\begin{aligned} f_3(y) &= \frac{2\alpha_s}{3\pi}\Big[(3-6y)\log\Big(\frac{y}{1-2y}\Big) + 2\log^2\Big(\frac{y}{1-y}\Big) + \frac{5}{2} \\ &\quad -6y - \frac{9}{2}y^2 + 4\mathrm{Li}_2\Big(\frac{y}{1-y}\Big) - \frac{\pi^2}{3}. \end{aligned} \tag{32}$$

The next-to-leading order corrections to f_3 have been calculated [15]. Because the hadronization corrections to f_3 are small, the three-jet rate provides one of the most precise measurements of α_s at LEP. A typical fit is shown in Fig.6 [13].

8 Heavy Quarkonium Decays

For the decay widths of ${}^3S_1$ $Q\overline{Q}$ quarkonium states, if $m_Q \gg \Lambda$ then the short- and long-distance effects can be factorized, with the former calculable in perturbative QCD. For the Υ [16],

$$\begin{aligned} \Gamma^{\mu^+\mu^-} &= \frac{4\pi}{9}\frac{|\psi(0)|^2}{m_b^2}\alpha^2\Big[1 - \frac{16}{3}\frac{\alpha_s}{\pi} + ...\Big] \\ \Gamma^{\gamma gg} &= \frac{32(\pi^2-9)}{81}\frac{|\psi(0)|^2}{m_b^2}\alpha\alpha_s^2\Big[1 - 7.4\frac{\alpha_s}{\pi} + ...\Big] \\ \Gamma^{ggg} &= \frac{40(\pi^2-9)}{81}\frac{|\psi(0)|^2}{m_b^2}\alpha_s^3\Big[1 - 4.9\frac{\alpha_s}{\pi} + ...\Big], \end{aligned} \tag{33}$$

in the $\overline{\mathrm{MS}}$ scheme with $\mu = m_b$.

The dependence on the wave function can be eliminated by forming *ratios*:

$$\begin{aligned} R_\mu \equiv \frac{\Gamma^{ggg}}{\Gamma^{\mu^+\mu^-}} &= \frac{10(\pi^2-9)}{9\pi}\frac{\alpha_s^3(\mu)}{\alpha^2}\Big[1 + (0.4 - 12.5\log\Big(\frac{m_b}{\mu}\Big))\frac{\alpha_s(\mu^2)}{\pi} + ...\Big] \\ R_\gamma \equiv \frac{\Gamma^{\gamma gg}}{\Gamma^{ggg}} &= \frac{4}{5}\frac{\alpha}{\alpha_s(\mu^2)}\Big[1 + (-2.6 + 4.2\log\Big(\frac{m_b}{\mu}\Big))\frac{\alpha_s(\mu^2)}{\pi} + ...\Big]. \end{aligned} \tag{34}$$

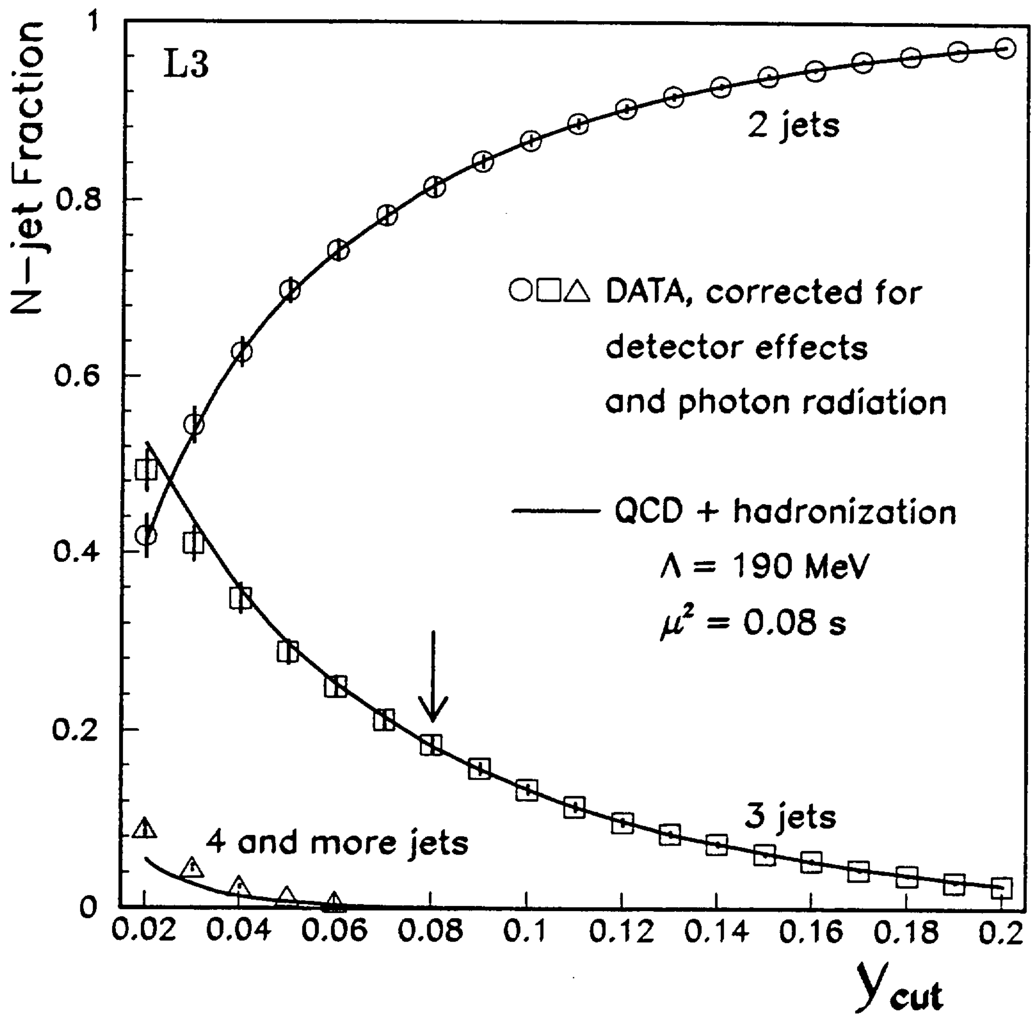

Figure 6: QCD fits to the jet rates at LEP as measured by the L3 collaboration, from reference [13].

In principle, R_γ provides a relatively clean measurement of α_s. In practice, there are non-negligible corrections from the photon acceptance and from non-relativistic effects. A more complete discussion can be found in reference [17].

A Cross-Section Formula

For a general $2 \to n$ scattering process $a + b \to c_1 + ... + c_n$ the cross section is

$$\sigma^{ab \to c_1 \dots c_n} = \frac{1}{F} \int_R d\Phi_n \, |\overline{M}^{ab \to c_1 \dots c_n}|^2, \tag{35}$$

where (i) F is the *flux factor*

$$F = 2\lambda^{\frac{1}{2}}(s, m_a^2, m_b^2) \lambda(x, y, z) = x^2 + y^2 + z^2 - 2xy - 2yz - 2zx, \tag{36}$$

(ii) $d\Phi_n$ is the Lorentz-invariant phase space volume element

$$d\Phi_n = \prod_{i=1}^{i=n} \frac{d^3 p_{c_i}}{(2\pi)^3 2E_{c_i}} (2\pi)^4 \delta^{(4)}(p_a + p_b - \sum_{i=1}^{i=n} p_{c_i}), \tag{37}$$

(iii) $\int_R$ specifies the allowed region of phase space integration, including where appropriate cuts on the final state momenta, and (iv) $|\overline{M}^{ab \to c_1 \dots c_n}|^2$ is the spin (and colour where appropriate) summed/averaged matrix element squared for the process $a + b \to c_1 + ... + c_n$.

B Parton Scattering Amplitudes

The following scattering amplitudes squared have been summed and averaged over final and initial state spins and colours. Not included are the overall coupling constants, g_s^4, $g_s^2 e_q^2$ and e_q^4 according to the number of strong and electromagnetic vertices.

$qq' \to qq'$	$\frac{4}{9}\frac{s^2+u^2}{t^2}$
$qq \to qq$	$\frac{4}{9}\left(\frac{s^2+u^2}{t^2} + \frac{s^2+t^2}{u^2}\right) - \frac{8}{27}\frac{s^2}{ut}$
$q\bar{q} \to q'\bar{q}'$	$\frac{4}{9}\frac{t^2+u^2}{s^2}$
$q\bar{q} \to q\bar{q}$	$\frac{4}{9}\left(\frac{s^2+u^2}{t^2} + \frac{t^2+u^2}{s^2}\right) - \frac{8}{27}\frac{u^2}{st}$

$$
\begin{array}{ll}
q\bar{q} \to gg & \dfrac{32}{27}\dfrac{u^2+t^2}{ut} - \dfrac{8}{3}\dfrac{u^2+t^2}{s^2} \\
gg \to q\bar{q} & \dfrac{1}{6}\dfrac{u^2+t^2}{ut} - \dfrac{3}{8}\dfrac{u^2+t^2}{s^2} \\
qg \to qg & \dfrac{u^2+s^2}{t^2} - \dfrac{4}{9}\dfrac{u^2+s^2}{us} \\
gg \to gg & \dfrac{9}{2}\left(3 - \dfrac{ut}{s^2} - \dfrac{us}{t^2} - \dfrac{st}{u^2}\right) \\
q\bar{q} \to \gamma g & \dfrac{8}{9}\dfrac{t^2+u^2}{ut} \\
qg \to \gamma q & \dfrac{1}{3}\dfrac{s^2+t^2}{-st} \\
q\bar{q} \to \gamma\gamma & \dfrac{2}{3}\dfrac{u^2+t^2}{ut} \\
q\bar{q} \to Q\overline{Q} & \dfrac{4}{9}\dfrac{(M^2-t)^2+(M^2-u)^2+2M^2s}{s^2} \\
gg \to Q\overline{Q} & \dfrac{1}{6}\left(\dfrac{(M^2-t)(M^2-u)-2M^2(M^2+t)}{(M^2-t)^2}\right. \\
& \qquad \left. + \dfrac{(M^2-t)(M^2-u)-2M^2(M^2+u)}{(M^2-u)^2}\right) \\
& + \dfrac{3}{4}\dfrac{(M^2-t)(M^2-u)}{s^2} - \dfrac{1}{24}\dfrac{M^2(s-4M^2)}{(M^2-t)(M^2-u)} \\
& - \dfrac{3}{8}\left(\dfrac{(M^2-t)(M^2-u)+M^2(u-t)}{s(M^2-t)}\right. \\
& \qquad \left. + \dfrac{(M^2-t)(M^2-u)+M^2(t-u)}{s(M^2-u)}\right).
\end{array}
\tag{38}
$$

References

[1] *Review of Particle Properties*, Phys. Lett. **239B** (1990) 1.

[2] W.J. Marciano, Phys. Rev. **D29** (1984) 580.

[3] J. Kwiecinski, A.D. Martin, R.G. Roberts and W.J. Stirling, Phys. Rev. **D42** (1990) 3645.

[4] G. Altarelli and G. Parisi, Nucl. Phys. **B126** (1977) 298.

[5] BCDMS collaboration: A.C. Benvenuti *et al.*, Phys. Lett. **237B** (1990) 592.

[6] G. Altarelli, R.K. Ellis and G. Martinelli, Nucl. Phys. **B143** (1978) 521; **B146** (1978) 544(e); **B147** (1979) 461.
J. Kubar-Andre and F.E. Paige, Phys. Rev. **D19** (1979) 221;
J. Kubar-Andre, M. Le Bellac, J.L. Meunier and G. Plaut, Nucl. Phys. **B175** (1980) 251.

[7] R. Hamberg, T. Matsuura and W.L. van Neerven, Nucl. Phys. **359** (1991) 343.

[8] P. Nason, S. Dawson and R.K. Ellis, Nucl. Phys. **B303** (1988) 607.
W. Beenakker *et al.*, Phys. Rev. **D40** (1989) 54.

[9] A. Djouadi, M. Spira and P.M. Zerwas, Phys. Lett. **264B** (1991) 440.

[10] S.D. Ellis, Z. Kunszt and D.E. Soper, Phys. Rev. Lett. **64** (1990) 2121; University of Washington preprint UW-PT-91-13 (1991).

[11] M. A. Samuel and L.R. Surguladze, Phys. Rev. Lett. **66** (1991) 560; **66** (1991) 2416(e).
S.G. Gorishny, A.L. Kataev and S.A. Larin, Phys. Lett. **259B** (1991) 144.

[12] B.A. Kniehl and J.H. Kuhn, Nucl. Phys. **B329** (1990) 547.

[13] T. Hebbeker, Plenary talk presented at the International Lepton-Photon Symposium and Europhysics Conference on High Energy Physics, Aachen preprint PITHA 91/17 (1991).

[14] JADE collaboration: S. Bethke *et al.*, Phys. Lett. **213B** (1988) 235.

[15] G. Kramer and B. Lampe, Fortschr. Phys. **37** (1989) 161.

[16] S.J. Brodsky, G.P. Lepage and P. Mackenzie, Phys. Rev. **D28** (1983) 228.
W.A. Bardeen, A.J. Buras, D.W. Duke and T. Muta, Phys. Rev **D18** (1978) 3998.

[17] K. Kwong *et al.*, Phys. Rev, **D37** (1988) 3210.